

TWO-DIMENSIONAL SIMULATION OF PYRITE OXIDATION AND POLLUTANT TRANSPORT IN BACKFILLED OPEN CUT COAL MINES

F. DOULATI ARDEJANI

Assistant Professor, Faculty of Mining and Geophysics, Shahrood University of Technology, Shahrood, *Iran*

R. N. SINGH

Professor of Mining Engineering, Faculty of Engineering, University of Wollongong, Northfields Avenue, Wollongong, NSW 2522, Australia. E-mail: raghu@uow.edu.au

Abstract

The spoil from backfilled open cut mines often contains pyrite which may be oxidised and produce acid mine drainage (AMD) if it is exposed to the atmosphere. AMD is often characterised by high concentrations of iron, high sulphate and low pH and it is considered to be a major cause of long-term poor water quality and is the source of many environmental problems. A numerical model that incorporates oxygen transport, pyrite oxidation, enthalpy balance, groundwater flow and transport of the oxidation products is presented to describe the long-term pyrite oxidation and pollutant leaching within the spoil of an open cut mine. A diffusion process governs the oxygen transport within the pore space of the backfill. A shrinking-core concept describes the oxidation of pyrite particles. The transport model incorporates physical processes (advection, diffusion) and chemical processes (ion exchange reaction). The ferric iron released by the chemical oxidation of ferrous iron and further produced by the bacterially catalysed reaction also participates in the pyrite oxidation reaction. The ferric iron precipitation and complexation reactions are allowed to take place during the course of its transport. A multi-purpose computational fluid dynamics (CFD) package called PHOENICS incorporating a finite volume numerical scheme has

been modified by creating a PHOENICS pre-processing input file in the PHOENICS input language (Q1_AMDOPCUTMI) and developing a subroutine called GROUND_ AMDOPCUTMI in the FORTRAN 99 language. The modeling accuracy was tested with the results obtained from the published numerical finite difference model. It was found that the oxidation of only a small fraction of pyrite is enough to generate an acid mine drainage load. Considerable pyrite creates a long-term source of acid mine drainage so that if no action is taken to reduce the acid generation and pollutant leaching, the receiving environments and water resources will be seriously damaged. The lowering of pH in the range between 2.5 to 3.5, results in the bacterial oxidation of pyrite being enhanced. Subsequently the bacterial action produces more Fe^{3+} , SO_4^{2-} , H^+ , and Fe^{2+} . The results clearly indicated that dissolved ferric iron remains above the water table while the ferrous iron peak appears below it, in the saturated zone. The simulation results can be used for designing effective site remediation programs in order to minimise environmental effects arising from abandoned backfilled open cut mines.

Introduction

Mining operations are often one of the most important causes of surface and groundwater pollution. These activities produce poor water quality and pose many environmental problems. Among the problems associated with mining activities, acid mine drainage (AMD) is more important and is considered to be a major cause of water pollution. In this paper a two-dimensional numerical finite volume model is presented for prediction of the long-term pyrite oxidation and subsequent pollutant transportation from backfilled open cut mines. The model incorporates oxygen transport, pyrite oxidation, enthalpy balance, groundwater flow and transport of the oxidation products. The model has been implemented in the general-purpose PHOENICS computational fluid dynamic package (Spalding, 1981; CHAM, 2000). By creating a Q1-file (PHOENICS input file) in PHOENICS input language, the necessary settings such as domain geometry, finite volume grid, boundary and initial conditions and fluid properties were specified and for all non-standard equations and specific source terms, the required coding in FORTRAN 99 language was supplied by developing a subroutine called GROUND. This subroutine was used by the PHOENICS solver module during the course of the solution. The conceptual model proposed in developing the model is given in Doulati Ardejani et al. (2002).

2. Modelling governing equations

2.1 Groundwater flow

The groundwater flow is based on the well recognised Laplace equation. This equation is obtained by coupling the continuity equation and Darcy's law. For a two-dimensional situation and under steady state conditions the governing equation for groundwater flow can be reduced as follows (Freeze and Cherry, 1979):

$$\frac{\partial}{\partial x_j} \left(K_{x_j} \frac{\partial h}{\partial x_j} \right) + W = 0 \quad (1)$$

where,

- $\sim x_j$ = Cartesian coordinates
- $\sim K_{x_i}$ = Directional hydraulic conductivity;
- $\sim h$ = hydraulic head;
- $\sim W$ = recharge or discharge rate per unit volume.

The components of the groundwater velocity were obtained by solving Equation 5 and were then used in the mass transport equation of any chemical species.

2.2 Pyrite oxidation mechanism

The oxidation of pyrite is well described by a shrinking core model (Levenspiel, 1972). This model can be modified to take into consideration spherical pyritic grains and incorporating both surface reaction kinetics and oxidant diffusion into the particles containing pyrite (Cathles and Apps, 1975):

$$\frac{\partial X}{\partial t} = \frac{-3 X^{\frac{2}{3}}}{6 \tau_{D_{[O_{2d}]}} X^{\frac{1}{3}} \left(1 - X^{\frac{1}{3}} \right) + \tau_{C_{[O_{2d}]}}} \quad (2)$$

where,

- $\sim X$ = fraction of pyrite remaining within the particle (Kg/Kg);
- $\sim t$ = time (s);

τ_c = total time required for complete oxidation of pyrite within a particle if the oxidation process is only

controlled by the decreasing surface area of pyrite (s);

τ_D = total time required for full oxidation of pyrite within a particle assuming the oxidation rate is solely

controlled by oxidant diffusion into the particles (s);

O_{xd} = oxidant.

τ_D and τ_c are expressed by Equations 7 and 8 (Levenspiel, 1972):

$$\tau_D = \frac{\rho_{Py} R^2}{6bD_{e[Ox]} C_{[Ox]}} \quad (3)$$

$$\tau_c = \frac{\rho_{Py} R}{bK_{[Ox]} \alpha_{Py}^{rock} \lambda C_{[Ox]}} \quad (4)$$

where,

ρ_{Py} = density of pyrite in the particle (mol / m^3);

R = particle radius (m);

b = stoichiometric ratio of pyrite to oxidant consumption (mol/mol);

$D_{e[Ox]}$ = effective diffusion coefficient of oxidant in oxidised rim of the particle (m^2 / s);

$K_{[Ox]}$ = first-order surface reaction rate constant (m/s);

α_{Py}^{rock} = surface area of pyrite per unit volume of particle (m^{-1});

λ = thickness of the particle in which pyrite oxidation occurs (reaction skin depth) (m);

$C_{[Ox]}$ = concentration of oxidant in the water surrounding the particle (mol / m^3).

2.3 Enthalpy equation

To model the heat transfer, a simple enthalpy balance is employed using Equation 9 (adopted from Cathles and Apps, 1975):

$$\rho_b C_p \frac{\partial T}{\partial t} = K_T \left(\frac{\partial^2 T}{\partial x_j^2} \right) - \rho_w C_w u_{x,w} \frac{\partial T}{\partial x_j} + \frac{3(1-\phi)B^{-1}\rho_s X^{\frac{2}{3}}}{6\tau_{D_{O_2}} X^{\frac{1}{3}} \left(1 - X^{\frac{1}{3}}\right) + \tau_{C_{O_2}}} + \frac{3(1-\phi)B'^{-1}\rho_s X^{\frac{2}{3}}}{6\tau_{D_{Fe^{3+}}} X^{\frac{1}{3}} \left(1 - X^{\frac{1}{3}}\right) + \tau_{C_{Fe^{3+}}}} \quad (5)$$

where,

- T = temperature ($^{\circ}C$);
- ρ_b = bulk density of the spoil (Kg/m^3);
- ρ_s = molar density of pyrite in spoil (mol/m^3);
- ϕ = porosity of spoil;
- K_T = thermal conductivity ($J/m^{\circ}CS$);
- C_p = specific heat capacity of the spoil ($J/kg^{\circ}C$);
- ρ_w = density of water in the spoil (Kg/m^3);
- $u_{x,w}$ = water velocity (m/s);
- C_w = heat capacity of water (spoil) ($J/kg^{\circ}C$);
- B = moles of pyrite consumed in pyrite-oxygen reaction per heat generated (mol/J);
- B' = moles of pyrite consumed in pyrite- Fe^{3+} reaction per heat generated (mol/J).

2.4 Oxygen balance

Oxygen is transported within the spoil of the open cut mines by the process of diffusion. It is consumed by the pyrite oxidation reaction, chemical oxidation of ferrous iron and bacteria (Jaynes et al. 1984a). The governing equation of oxygen transport incorporating the volumetric consumption terms reduces to:

$$\phi_a \frac{\partial u}{\partial t} = D_e \left(\frac{\partial^2 u}{\partial x_j^2} \right) - S_{K_{Py-O_2}} - S_{K_{Fe^{2+}-O_2}} - S_{K_{B-O_2}} \quad (6)$$

where,

- ϕ_a = air-filled porosity of the spoil (m^3/m^3);
- u = oxygen in the spoil pore space (mol/m^3);

D_e = effective diffusion coefficient (m^2 / s);

$S_{K_{Py-O_2}}, S_{K_{Fe^{2+}-O_2}}, S_{K_{B-O_2}}$ = volumetric oxygen consumption terms ($mol / m^3 s$) by

the pyrite oxidation reaction, chemical oxidation of ferrous iron and oxygen consumption by bacteria. The oxygen consumption terms can be found in Jaynes et al. (1984a) and modified by Doulati Ardejani et al. (2002).

2.5 Transport equation

The oxidation products are transported through the groundwater flow system after leaching from the spoil. The governing transport equation can be expressed as follows (Rubin and James, 1973; Freeze and Cherry, 1979):

$$\phi \frac{\partial C_i}{\partial t} + \rho_b \frac{\partial \bar{C}_i}{\partial t} = D \frac{\partial^2 C_i}{\partial x_j^2} - q_j \frac{\partial C_i}{\partial x_j} + q_{re} C_i \pm S \quad i = 1, 2, \dots, n_c \quad (7)$$

where,

C_i = solute concentration in aqueous form (mol / m^3);

\bar{C}_i = solute concentration in adsorbed form (mol / Kg);

ρ_b = bulk density of the medium (Kg / m^3);

q_{re} = surface recharge (m / s);

S = sink and source terms representing the changes in aqueous component concentrations due to the chemical reactions ($mol / m^3 s$);

q_j = vector components of the pore fluid specific discharge (m / s);

D = hydrodynamic dispersion coefficient (m^2 / s).

3. Modelling input parameters

The model input data were taken from Cathles and Apps (1975) and Jaynes et al. (1984b) in order to perform one and two-dimensional simulations. The one-dimensional simulation was run to verify modelling accuracy and then a two-dimensional simulation was carried out when the reasonable output results were obtained in comparison with those results obtained from the POLS finite difference model developed by Jaynes et al. (1984a, b). For simulation purpose, the PHOENICS package was modified. The model input parameters are given in Table 1.

4. Model calibration

One-dimensional simulation was carried out to calibrate the model and verify the capability of the model for simulation of pyrite oxidation and leaching process associated with open cut coal mines. To perform a one-dimensional simulation, a 10-metre spoil column was simulated as 20 equal size control volumes. The influx and background concentrations of dissolved species and pH are listed in Table 2.

A first type boundary condition was assigned at the top of the spoil profile for the oxygen transport model equal to its atmospheric concentration (9 mol/m^3). The spoil column initially contained no oxygen concentration. A zero-gradient boundary condition was considered at the profile base.

The following boundary conditions were assigned for the enthalpy model. The spoil temperature was initially set at 15°C as follows:

$$T(x_j, 0) = 15^\circ\text{C} \quad (8)$$

The top surface of the spoil profile was specified as a first type boundary condition equal to 15°C :

$$T(0, t) = 15^\circ\text{C} \quad (9)$$

A constant recharge of $2 \times 10^{-8} \text{ m/s}$ was maintained at the profile top surface. A dispersivity of 0.005 m was applied for the transport model in order to achieve consistency with the POLS model. The main reason of selecting a small value of dispersivity is that the mechanism of the leaching process used in the POLS model is different from the present finite volume model. The POLS model did not consider the processes of diffusion and hydrodynamic dispersion effects. The following boundary and initial conditions were specified for the transport of the oxidation products:

The top boundary of the model was assigned as first type with respect to concentration of solutes

The background solute concentrations were simulated by specifying an initial boundary condition

A zero concentration gradient boundary condition was specified at outflow boundary.

Table 1.

Parameters used for simulation (Jaynes et al., 1984b; Cathles and Apps, 1975)

Parameter	Value
Pyrite fraction spoil	$0.0025 \text{ Kg pyrite/ Kg}$

Fraction coarse particles containing pyrite	75 %
The bulk density of spoil	1650
Kg / m^3	
The porosity of the spoil	0.321
Water-filled porosity	0.225
Surface area of pyrite per unit volume of spoil	80 cm^{-1}
Radius of particles	2 cm
Diffusion coefficient of oxidant in water	
$1.0 \times 10^{-11} m^2 / s$	
Molar density of pyrite within particle	23
mol / m^3	
First-order rate constant for Fe^{3+}	
$4.4 \times 10^{-8} m / s$	
First-order rate constant for oxygen	
$8.3 \times 10^{-10} m / s$	
Recharge value	0.5
m / yr	
constants for chemical oxidation of Fe^{2+}	
$K_1 = 1.3 \times 10^{-10} (mol^2 / (m^3)^2 (s))$	
$K_2 = 1.7 \times 10^{-9} s^{-1}$	
Effective diffusion coefficient for oxygen transport	
$1.0 \times 10^{-7} m^2 / s$	
Enthalpy of Reaction (1)	
$-1.45 \times 10^6 J / mol$ (CRC, 1998)	
Enthalpy of Reaction (3)	
$-1.78 \times 10^4 J / mol$ (CRC, 1998)	
Moles of pyrite consumed per heat generated in $FeS_2 - O_2$ reaction	
$6.9 \times 10^{-7} mol / J$	
Moles of pyrite consumed per heat generated in $FeS_2 - Fe^{3+}$ reaction	
$5.6 \times 10^{-5} mol / J$	
Thermal conductivity	2.1
$J / m^{\circ}CS$	
Specific heat capacity	2500
$J / Kg^{\circ}C$	

Table 2.

Influx and background chemistry (Jaynes et al., 1984b)

Aqueous components	concentration (mol / m^3)
Influx data:	
Fe^{2+}	0.0
Fe^{3+}	0.0
SO_4^{2-}	50
pH	5
Background data:	
Fe^{2+}	0.5
Fe^{3+}	0.0
SO_4^{2-}	50
pH	5

4.1 One-dimensional simulation results

For one-dimensional simulation, the effective diffusion coefficient for oxygen transport was selected to be $1.0 \times 10^{-7} m^2 / s$ and air-filled porosity of 0.1 was set for the simulation. The temperature rise due to the pyrite oxidation reactions was ignored and a constant temperature equal to $15^\circ C$ was considered for modelling purposes. The iron-oxidising bacteria were allowed to be active in the spoil profile where the conditions were favourable. The mathematical expressions describing the role of bacteria were taken from Jaynes et al. (1984a) and relevant FORTRAN codes were supplied in the GROUND subroutine accessible by the user of the PHOENICS package. The interaction between H^+ produced by oxidation reactions and spoil was incorporated by a simple empirical relationship (Jaynes et al. 1984a):

$$\frac{H^+}{H_{Gen}^+} = \{1.0 - EXP(G_A - pH)\} \quad (10)$$

where,

H^+ = Hydrogen ion in solution (mol / m^3);

H_{Gen}^+ = H^+ generated through chemical reactions (mol / m^3);

G_A = an empirical constant that defines the buffer system.

In this paper, Equation 14 was slightly modified to calculate the H^+ consumption per cubic metre of spoil per unit time as given below:

$$\frac{\partial H^+}{\partial t} = -\frac{H_{Gen}^+}{\Delta t} \exp(G_A - pH) \quad (11)$$

where,

Δt = simulation time step (s).

Equation 15 was incorporated as a sink term in the governing transport equation for the hydrogen ion. In this particular case the solution pH was maintained above 2.5. No ferric iron complexation reaction was considered in this simulation.

The H^+ - spoil interaction increased the pH of the solution. It caused an increase in the bacterial activity therefore more ferric iron was produced. Consequently, the pyrite oxidation rate increased considerably over time (Fig. 1). As Fig. 1 shows, about 29 % of the pyrite was oxidised after 10000 days of the simulation. For this time, the POLS model predicted that 30.5 % of pyrite was consumed. The difference between the finite volume modelling predictions and those predicted by the POLS model can be explained in that unlike the POLS model, the ferric complexation reaction was not incorporated in the finite volume model. The complexation reaction increases the ferric concentration. Consequently the rate of pyrite oxidation increases.

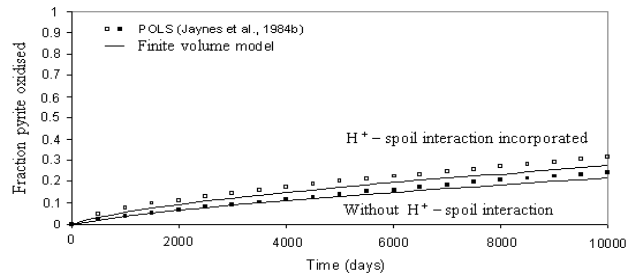


Fig. 1. Comparison of the POLS results (dots) with the PHOENICS results (solid lines) for the pyrite oxidised vs. time over entire spoil column with and without H^+ - spoil interaction.

The mole fraction of oxygen within the spoil profile versus depth was illustrated in Fig. 2. Oxygen decreased linearly with depth. As Fig. 2 shows, oxygen diffusion was limited in the surface elements of the spoil profile up to 2.5 metres from the spoil surface. Bacterial activity ($S_{K_{B-O_2}}$ in Eq. 10) was the main reason for this sharp reduction of oxygen concentration within the surface layers of the spoil profile, consuming most of the oxygen over this part of the profile.

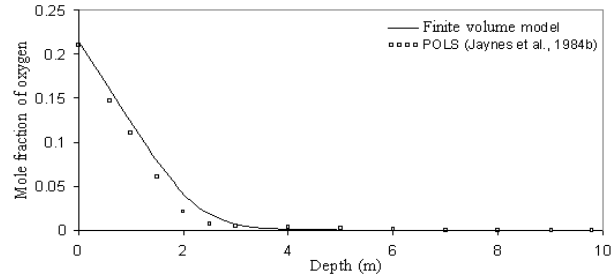


Fig. 2. Comparison of the POLS modelling results (dots) with the finite volume simulated results (solid lines) for oxygen mole fraction as a function of depth for 5-year period.

Fig. 3 shows the total iron-discharging rate as a function of time predicted in the water leaving the spoil profile for two different cases. In Case 1 the iron-oxidising bacteria are active and the interaction between the spoil and H^+ is incorporated. In Case 2 no bacteria are allowed to be present but in this case the effective diffusion coefficient for oxygen transport is four times greater than that in Case 1. A comparison was made with those results predicted by the POLS model (dots). The iron-leaching rate showed a similar pattern with time for both cases and the maximum rate occurred between 1750 to 2100 days. As Fig. 3 shows, the leaching rate in Case 2 is greater than in case 1 due to bigger in the effective diffusion coefficient.

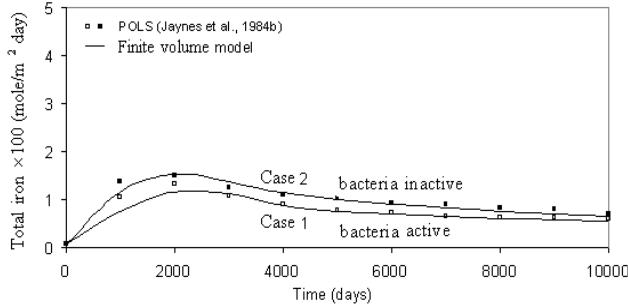


Fig. 3. Total iron leaching rate vs. time in the water leaving the spoil profile for Cases 1 and 2.

The difference in head between the left and the right boundaries was maintained at 0.1 m. An average recharge value of 0.3 m/yr was considered for the upper boundary (spoil surface). For the simulation it was assumed that reactive pyrite was contained only in a 12.5-m-wide segment of the unsaturated zone of the spoil (Fig. 4a).

The upper 4 m of the grid was assumed to be unsaturated and the remainder fully saturated with a constant porosity of 0.321. For simplicity the horizontal component of the velocity was ignored in the unsaturated zone and flow was only assumed to be vertical in this zone. Horizontal and vertical hydraulic con-

ductivities of 1.50×10^{-5} m/s and 1.50×10^{-6} m/s were used for the simulation. Horizontal and vertical dispersion coefficients of 7.0×10^{-9} m²/s and 5.0×10^{-9}

5. Two-dimensional simulation

5.1 Modelling setting and input data

Two-dimensional simulations were also performed to demonstrate the capability of the finite volume model for prediction of the long-term pyrite oxidation and transportation of the oxidation products from backfilled open cut coalmines. The input parameters are similar to those input data used for one-dimensional simulation (Table 1) but slight modification was made to the influx and background chemistry of the aqueous components. Chemical species considered in the two-dimensional simulations are the same as those in the one-dimensional model. These chemical species with their influx and background concentrations are listed in Table 3.

Table 3.

Source and background concentrations of aqueous components used for 2-D simulations

Component	Concentration	
	Source <i>mol / m³</i>	Background <i>mol / m³</i>
Fe^{2+}	5.00×10^{-1}	5.00×10^{-1}
Fe^{3+}	2.00×10^{-5}	0
SO_4^{-2}	5.00×10^1	5.00×10^1
<i>pH</i>	4	5

The two-dimensional cross-sectional dimensions are 50 m horizontally by 20 m vertically and this domain is discretised into 40×20 control volumes of size

1.25 m horizontally x 1m vertically. m^2/s were specified for the model. The steady state flow system in terms of velocity vectors is given in Fig. 4b.

The spoil temperature was assumed constant at 15 °C and the temperature rise in pore water due to the oxidation reactions was predicted using the enthalpy balance. An effective diffusion coefficient of $2.0 \times 10^{-7} m^2/s$ was assigned for the oxygen transport model. The bacterial action and the interaction between H^+ and the spoil were also considered for two-dimensional simulation. The spoil surface was maintained as a first-type boundary condition for oxygen equal to its atmospheric concentration ($9 mol/m^3 \approx 0.21 mol/mol$). First – type boundary conditions were specified above the water table for the oxygen transport model. The spoil solution initially contained no oxygen. To avoid non-linearity problems, no ferric complexation reactions were allowed to take place. The ferric precipitation reaction was incorporated for 2-D simulations. An oxidation period of 10000 days (≈ 27 years) was considered for the simulation.

The pH of the system was not allowed to drop below 2.5. The interaction between H^+ and the spoil and also maintaining the pH closer to the optimum pH required for the maximum activity of the iron-oxidising bacteria (≈ 3), caused more ferric iron to be produced by the bacterially mediated oxidation of ferrous iron. Consequently more pyrite was oxidised.

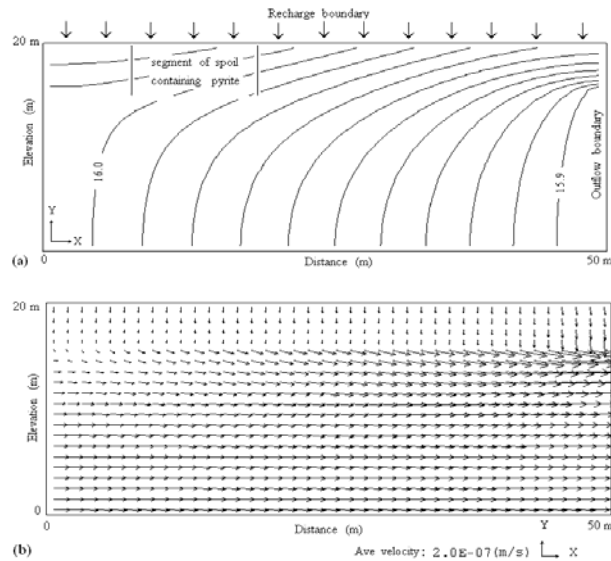


Fig. 4. Two-dimensional simulation cross-section: (a) hydraulic head and the segment of the spoil where oxidation reactions take place; (b) velocity vectors.

Fig. 5 shows the oxygen concentration for a 5-year-period of the simulation. In the segment where chemical reactions take place, more oxygen was consumed due to bacterial activity.

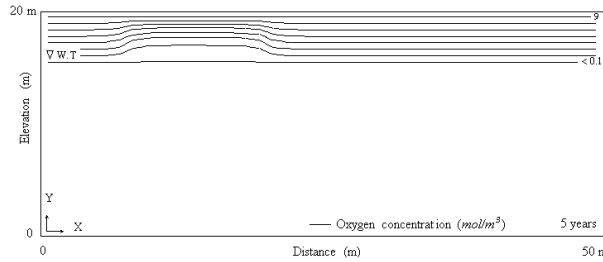


Fig 5. Oxygen concentration after 5 years of simulation.

The ferrous iron concentrations for simulation times of 5 and 10 years were illustrated in Fig. 6. After 5 years of the simulation (Fig. 6a), pH reached about 5, a favourable pH required for bacterial activity. The bacteria catalysed the ferrous iron oxidation reaction and more Fe^{2+} converted to Fe^{3+} . Therefore, the ferrous iron concentration decreased in the unsaturated zone whereas the ferric iron concentrations increased considerably in this zone.

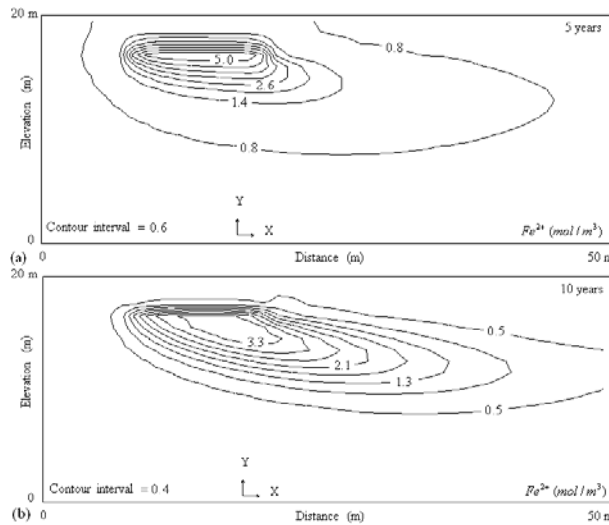


Fig. 6. Fe^{2+} concentration after: (a) 5 years; (b) 10 years of simulation.

After 10 years of the simulation (Fig. 6b), pH is still in the range that is favourable for bacterial activity; therefore, low concentrations of ferrous iron are seen in the unsaturated zone where the ferric concentration is dominant and a peak Fe^{2+} concentration is seen in the saturated zone.

Fig. 7 shows the solution pH for simulation times of 5 years and 10 years respectively. As pyrite oxidation takes place the pH dropped significantly (average pH is 3 in the unsaturated zone) but it never drops below about 2.5 due to the reaction between the spoil and H^+ . By 10 years the average pH is about 3.5 in the unsaturated zone due to the transport of hydrogen ions downward by the water flow.

Fig. 8a shows the ferric iron concentration after 5 years of simulation. The concentrations of Fe^{3+} are high in the unsaturated zone where oxygen is available and the conditions for maximum bacterial activity are favourable. The ferric ion concentrations are limited to the unsaturated zone, but as time progresses (Fig. 8b) some is being transported below the water table. In the case where pyrite is present below the water table, Fe^{3+} is converted back into Fe^{2+} through the Fe^{3+} - pyrite reaction. By incorporating the ferric iron precipitation reaction (Fig. 8c), aqueous ferric iron was removed from the solution phase in the saturated zone where the pH is greater than 3.5.

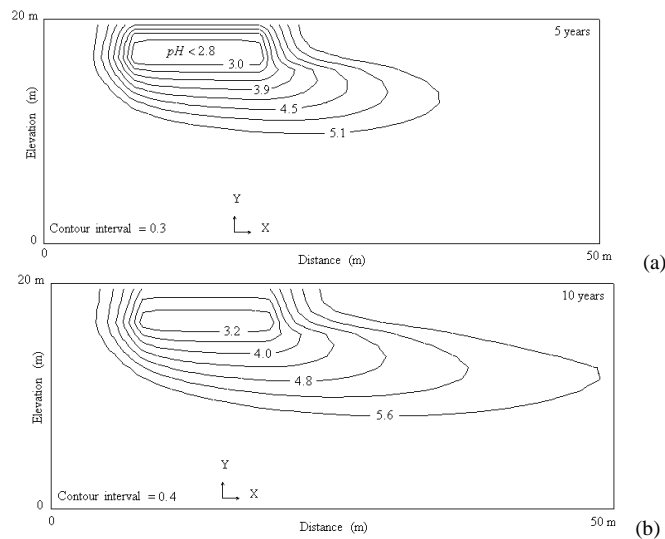


Fig. 7. pH after: (a) 5 years; (b) 10 years of simulation.

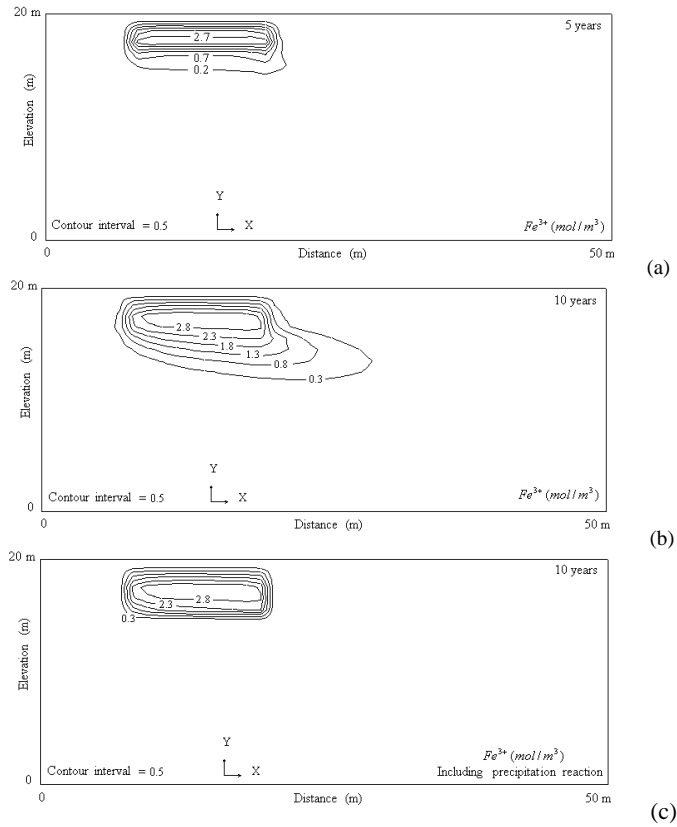
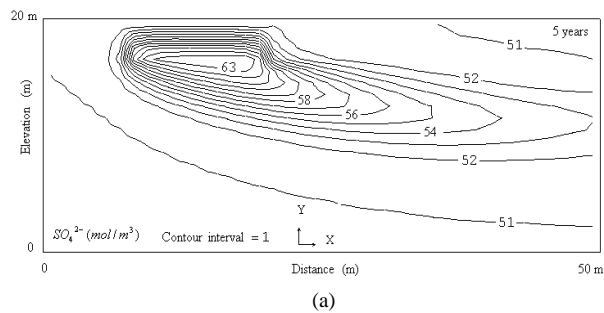


Fig. 8. Fe^{3+} concentration after: (a) 5 years; (b) 10 years (without precipitation reaction); (c) 10 years (including precipitation reaction) of simulation.

Fig. 9 shows SO_4^{2-} concentrations for time periods of 5 and 10 years. Considerable amounts of SO_4^{2-} were produced due to the fact that both oxygen and Fe^{3+} react with pyrite and higher SO_4^{2-} concentrations are produced.



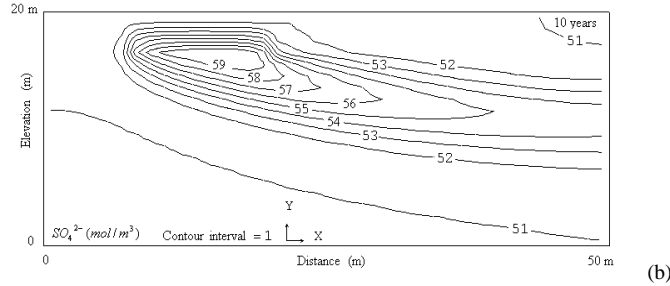
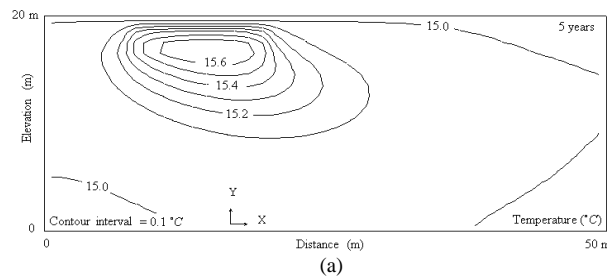


Fig. 9. SO_4^{2-} concentration after: (a) 5 years; (b) 10 years of simulation.

Although not illustrated, early in the simulation the SO_4^{2-} peak occurs in the unsaturated zone. Pyrite-oxygen reaction is recognised to be the only important source for SO_4^{2-} production at the beginning of the simulation.

At 5 years (Fig. 9a), an SO_4^{2-} peak (greater than 63 mol/m^3) occurred in the saturated zone due to a downward recharge water flow. In the saturated zone, SO_4^{2-} spreads by groundwater flow. By 10 years (Fig. 9b), the SO_4^{2-} peak moved further down into the saturated zone to about 6 metres depth, whereas SO_4^{2-} concentrations in the unsaturated zone began to decrease. No significant concentrations of SO_4^{2-} were produced in the saturated zone by the reaction between ferric iron and pyrite, because, for two-dimensional simulations, it was considered that only pyrite in a 12.5 m wide segment of the unsaturated zone participates in the oxidation reaction.

Fig. 10 shows the temperature distribution within the spoil section predicted after 5 and 10 years of simulations, respectively. No iron-oxidising bacteria are considered for obtaining these results. As this figure shows in the zone where the pyrite oxidation reaction takes place, the temperature rose from a background spoil temperature equal to 15°C to a maximum value of more than 15.6°C . This maximum temperature decreased to 15.5°C after 10 years of the simulation.



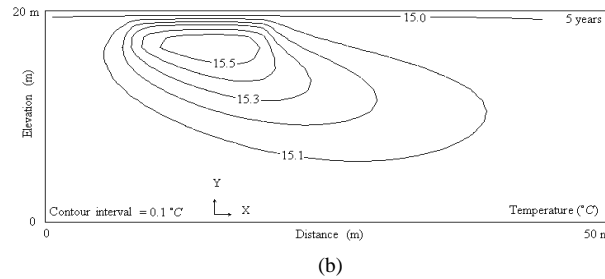


Fig. 10. Temperature rise after: (a) 5 years; (b) 10 years of the simulation.

6. CONCLUSIONS

A numerical finite volume model has been developed by modification of a computational fluid dynamics (CFD) package called PHOENICS to simulate long-term pyrite oxidation and pollutant generation within the spoil of an open cut mine. The results of two-dimensional simulations indicate:

Bacterial activity caused a sharp depletion of oxygen in the vadose zone.

The oxidation of only a small fraction of pyrite is enough to generate an acid mine drainage load. Considerable pyrite presence creates a long-term source of acid mine drainage.

The lowering of pH in the range between 2.5 to 3.5, results in the bacterial oxidation of pyrite being enhanced. Subsequently the bacterial action produces more Fe^{3+} , SO_4^{2-} , H^+ , and Fe^{2+} .

The results of two-dimensional simulations clearly indicate that dissolved ferric iron remains above water table while a ferrous iron peak appears below it, in the saturated zone.

Sulphate initially generated by the pyrite-oxygen reaction and subsequent production from the Fe^{3+} -pyrite reaction due to bacterial action mainly has its peak below the water table.

The results of the 2-D simulations can be used for designing effective site remediation programs in order to minimise environmental effects arising from abandoned backfilled open cut coalmines.

Acknowledgements

The authors wish to express their deep appreciation to Dr. Joe Shonhardt, for his contribution in preparation of this paper. The assistance provided by the Shahrood University of Technology and the Faculty of Engineering, University of Wollongong are also acknowledged.

References.

Cathles, L.M. and Apps, J.A. (1975). A model of the dump leaching process that incorporates oxygen balance, heat balance and air convection. *Metallurgical Transactions B*. Volume 6B, pp.617-624.

CHAM (2000). The PHOENICS On-Line Information System,
http://www.cham.co.uk/phoenics/d_polis/polis.htm

Chen, M., Soulsby, C. and Younger, P.L. (1999). Modelling the evolution of mine water pollution at Polkemmet Colliery, Almond catchment, Scotland. *Quarterly Journal of Engineering Geology*, 32(4), pp. 351-362.

CRC, Handbook of chemistry and physics, D.R., Lide (Editor-in-chief), 78th edition, CRC press LLC, Boca Roton, New York, 1997-1998.

Doulati Ardejani, F., Singh, R.N. and Baafi, E.Y. (2002). A numerical finite volume model for prediction of pollution potential of open cut mine backfill. 6th Annual Environmental Engineering Research Event 2002 conference, Blackheath NSW, Australia, ISBN: 0-9580158-1-3.

Elberling, B., Nicholson, R.V. and Scharer, J.M. (1994). A combined kinetic and diffusion model for pyrite oxidation in tailings: a change in controls with time. *Journal of Hydrology*, 157(1), pp.47-60.

Freeze, R.A. and Cherry, J.A. (1979). *Groundwater*, Prentice-Hall, Inc., Englewood Cliffs, New Jersey, 604p.

Guedes de Carvalho, R.A., Gonzalez Bega, C.G., Martins Sampaio, M.N., Neves, O. and Sol pereira, M.C. (1986). A study of the drainage of the pyrite mines of Aljustrel (Portugal). *International Journal of Mine Water*, 5(2), pp. 43-56.

Jaynes, D.B., Rogowski, A.S. and Pionke, H.B., (1984a). Acid mine drainage from reclaimed coal strip mines, 1, Model description. *Water Resources Research*, 20 (2), pp.233-242.

Jaynes, D.B., Rogowski, A.S. and Pionke, H.B., (1984b). Acid mine drainage from reclaimed coal strip mines, 2, Simulation results of model. *Water Resources Research*, 20 (2), pp.243-250.

Levenspiel, O. (1972). Chemical reaction engineering, John Wiley, New York, 578p.

Rogowski, A.S., Pionke, H.B., and Broyan, J.G. (1977). Modelling the impact of strip mining and reclamation processes on quality and quantity of water in mined areas: A review. *Journal of Environmental Quality*, 6 (3), pp.237-244.

Rubin, J. and James, R.V. (1973). Dispersion-affected transport of reacting solutes in saturated porous media: Galerkin method applied to equilibrium-controlled exchange in unidirectional steady water flow. *Water Resources Research*, 9 (5), pp.1332-1356.

Spalding, D.B. (1981). A general purpose computer program for multi-dimensional one- and two-phase flow. *Mathematics and Computers in Simulation*, 23(3), pp.267-276.

Walter, A.L., Frind, E.O., Blowes, D.W., Ptacek, C.J. and Molson, J.W. (1994a). Modelling of multi-component reactive transport in groundwater, 1, Model development and evaluation. *Water Resources Research*, 30(11), pp.3137-3148.

Walter, A.L., Frind, E.O., Blowes, D.W., Ptacek, C.J. and Molson, J.W. (1994b). Modelling of multicomponent reactive transport in groundwater, 2, Metal mobility in aquifers impacted by acidic mine tailings discharge. *Water Resources Research*, 30(11), pp.3149-3158.

Wunderly, M.D., Blowes, D.W., Frind, E.O. and Ptacek, C.J. (1996). Sulfide mineral oxidation and subsequent reactive transport of oxidation products in mine tailings impoundments: A numerical model. *Water Resources Research*, 32 (10), pp.3173-3187.